symmetric patterns with low sidelobe levels are made available by this technique.

A highly efficient multiple frequency paraboloid reflector antenna feed system can be realized by employing a multiplicity of coaxial conical horn radiators, with suitable radial aperture reactive tuning elements provided in each individual feed aperture annulus.

References

[1] L. A. Kraus and C. E. Profera, "Radiation from an iris terminated coaxial waveguide," in *1972 Int. IEEE/G-AP Symposium Digest.*
[2] C. E. Profera, "A comparison between analytic and experimental techniques for studying radiation from an open ended and iris terminated coaxial waveguide," Ph.D. dissertation, Drexel University, Philadelphia, Pa., Apr. 1973.
[3] N. Marcuvitz, *Waveguide Handbook.* New York: McGraw-Hill, 1951.
[4] S. Silver, *Microwave Antenna Theory and Design.* New York: McGraw-Hill, 1949.

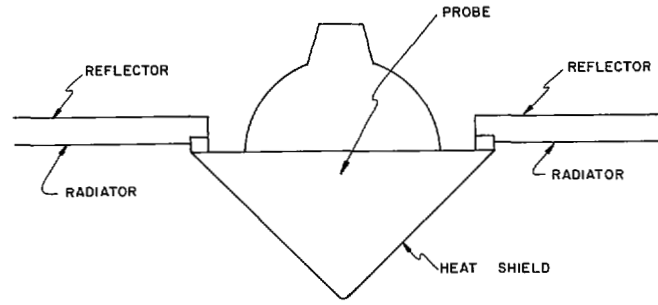

Fig. 1. Physical layout of probe.

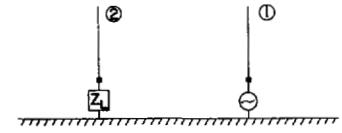

Fig. 2. Antenna model.

A Radio Altimeter Antenna for a Planetary Probe

JAMES B. BEYER, MEMBER, IEEE, JURIS AFANASJEVS, MEMBER, IEEE, AND NADAV LEVANON, MEMBER, IEEE

***Abstract*—The design of a 400 MHz directional antenna for a space vehicle is presented. The design utilizes the spacecraft itself as an integral part of the antenna. The antenna has a gain of 4 dB over a dipole, a front to back ratio of 8 dB, and a −6 dB beam angle of 34°. Design equations and experimental data are presented.**

Introduction

The antenna design presented in this paper resulted from the need to develop a directive radio altimeter antenna for tentative use in a freely-falling probe in a planetary atmosphere. Radiation considerations make a physically large antenna preferable to exploit the dependence of the return power on the square of the wavelength λ. The inviolate requirement of the probe heat shield and probe launching considerations dictated a deployable antenna stowed behind the heat shield during the primary phase of penetration of the planetary atmosphere. The electrical requirement, imposed by the power available and system noise, is that the gain in the direction of the probe cone axis be at least 3 dB over a dipole. The altimeter application imposes the requirement of linear polarization. The design necessary to satisfy the above criteria includes the heat shield as an integral part of the antenna and is presented in the following.

Theoretical Considerations

In order to achieve the gain and directivity required of the antenna, an array of at least two elements is needed. Dipole elements are made impractical because of the proximity of the heat shield, hence monopole elements using the heat shield as the ground plane are used. Because these elements must be located at the after edge of the heat shield and because radiation to the rear of the probe is not useful to the radio altimeter, a parasitic element is placed behind the driven element to increase both the front to back ratio and the directive gain. A typical physical layout of the probe including a sketch of the monopole-parasitic array is shown in Fig. 1.

Fig. 1 indicates that because of the mechanical construction of the probe it is necessary to support the parasitic element by a short length of conductor normal to the parasitic element. This length of conductor proves to be advantageous electrically because it serves as a reactive load for the parasitic element, and adjustment of this length plays a crucial role in determining the phase and amplitude of the parasitic element current.

The approximate behavior of a single driven element and its parasitic may be determined from the model shown in Fig. 2. Element 1 is the driven element and element 2 is the parasitic with terminating impedance Z_L resulting from the support conductor. For such a system the determining equations can be written as

$$V_1 = I_1 Z_{11} + I_2 Z_{12} \quad \text{and} \quad 0 = I_1 Z_{21} + I_2 (Z_{22} + Z_L). \tag{1}$$

For a parasitic of length equal to that of the driven element we take $Z_{11} = Z_{22}$, and of course $Z_{12} = Z_{21}$. As a result

$$\frac{I_2}{I_1} = \frac{-Z_{12}}{Z_{11} + Z_L}. \tag{2}$$

The current ratio I_2/I_1 is thus affected by a change in parasitic to driven element spacing not only through the change in Z_{12} but by the change in Z_L as well. The use of (2) as a design equation is complicated by the fact that Z_{12} and Z_{11} are not readily calculable due to the complex geometry presented by the probe. However, Z_L can be calculated, Z_{11} measured directly, and Z_{12} measured indirectly. Data from these measurements predict radiation patterns which were verified experimentally, as will be shown later.

The complete antenna may be considered to be an array of two collinear elements, each element as described above, consisting of a driven radiator and its parasitic. The composite radiation pattern will thus be the product of a) the pattern of a quarter wave monopole above a ground plane, b) the array factor of such

Manuscript received August 4, 1975. This work was supported under NASA Contract NAS5-8015.
J. B. Beyer is with the Department of Electrical and Computer Engineering, University of Wisconsin, Madison, WI 53706.
J. Afanasjevs is with the Space Science and Engineering Center, University of Wisconsin, Madison, WI 53706.
N. Levanon is with the Department of Environmental Sciences, Tel-Aviv University, Tel-Aviv, Israel.

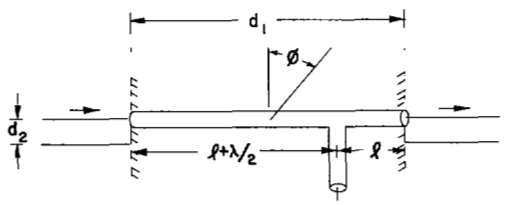

Fig. 3. Array drive system.

a radiator and a parasitic, hereafter called $|AF_1|$, and c) $|AF_2|$, the array factor for the two element array [1] given by

$$AF_2 = \frac{1}{2}\frac{\sin \psi}{\sin (\psi/2)} \tag{3}$$

where

$$\psi = \beta d \sin \theta$$

and

- $\beta = 2\pi/\lambda$
- d element spacing
- θ polar angle measured from a reference line normal to the array axis.

Experimental Results

A design frequency of 400 MHz was chosen for the antenna because the radio altimeter of interest [2] operates near this frequency and because the probe cone base diameter corresponds roughly to a wavelength at this frequency. Due to the lack of impedance data at 400 MHz, initial experiments were carried out on a 1/25 scale model at 10 GHz. The use of an indoor microwave antenna range and an available supply of instrumentation facilitated the numerous experiments and refinements which led to the final model. The probe model shown in Fig. 3 was used as a transmitting antenna driven by a stabilized 10 GHz source while a standard gain horn, fixed in position, connected to a superheterodyne system, served as the receiver. In this manner experiments for evaluating the effects of element spacing, length, and tilt angle with respect to the probe axis were readily carried out.

The two active elements of the array must be fed with currents having the same phase in order to obtain a radiation maximum at $\theta = 0°$. This was accomplished by inserting a $\lambda/2$ phasing section in series with one of the drive lines as indicated in Fig. 3. In order to verify (3), experiments were carried out using only driven monopoles as the array elements. The measured radiation patterns indicated that the individual element patterns are closely approximated by a cos θ dependence, and the effective element spacing should be taken as 1.18 λ rather than the actual spacing of 1.02 λ. Using these values, which give nulls at $\pm 25°$ and minor lobes at $\pm 52.5°$, accounts rather well for the irregularly shaped ground plane.

Experiments designed to optimize the parasitic element spacing and length indicate a spacing on the 10 GHz model of $\lambda/15$ and a length equal to that of the driven element. The radiation pattern of such an array is shown in Fig. 4. The -6 dB beam angle is 34°, the front to back ratio is 10 dB, and the antenna has a directive gain of 3.95 dB compared to a one-half wavelength dipole. The nulls in the forward pattern at $\pm 25°$, which gave rise to the effective spacing mentioned above, can also be seen in this figure. Since impedance measurements were impractical on the 10 GHz model, they were made on a full size 400 MHz antenna. The construction of this array was

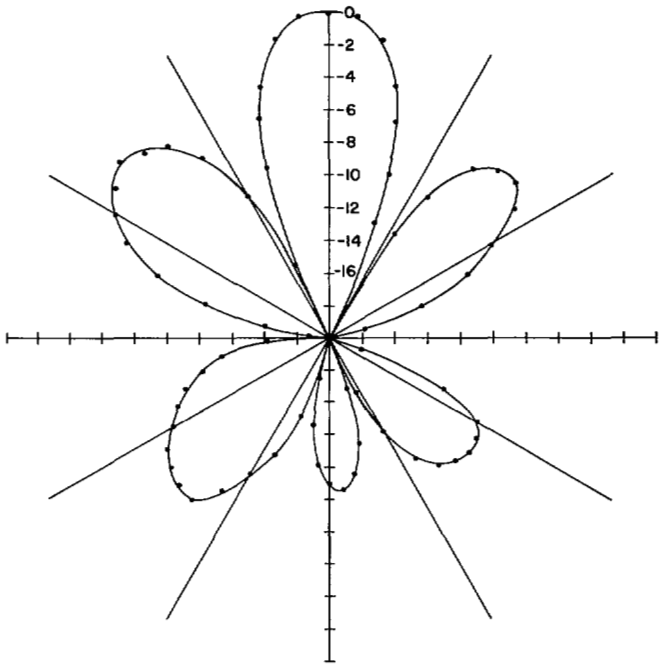

Fig. 4. Radiation pattern of 10 GHz model.

dictated by the results obtained with the 10 GHz model. The impedance measurements yielded a value of $Z_{11} = 91\angle 0° \Omega$ and an input impedance of a monopole element and its parasitic, that is, of the structure of Fig. 2, of $Z_{IN} = 81\angle 48° \Omega$. Solving (1) for the ratio $V_1/I_1 = Z_{IN}$ and rearranging yields

$$Z_{12} = \sqrt{{Z_{11}}^2 - Z_{IN}(Z_{11} + Z_L)}. \tag{4}$$

Calculating the parasitic element load impedance from [3]

$$Z_L = j\frac{\mu_0 \omega}{2\pi} \ln \frac{\lambda}{2\pi a} \tag{5}$$

where a = conductor radius, yields a value of $j40\ \Omega$. Using this value in (2) and (4) gives the parasitic to driven element current ratio $I_2/I_1 = 0.97\angle 130°$. The array factor for these two elements previously called AF_1 can now be determined from

$$|AF_1| = K|1 + Ae^{j(\Phi - \beta d_2 \sin \theta)}| \tag{6}$$

where

- K constant
- $A = |I_2/I_1|$
- Φ lead of I_2 with respect to I_1
- d_2 driven element to parasitic spacing
- θ polar angle measured from reference normal to elements.

Use of (3) and (6) then allows calculation of the radiation pattern of the composite array and the results are shown in Fig. 5 along with the measured pattern at 400 MHz.

Conclusions

As evidenced by the results shown in Fig. 5, the original design goals are met by this array which has a gain of 4 dB over a dipole and a front to back ratio of 8 dB. Furthermore, design equations are presented, which, along with experimentally obtained impedance data can be used to modify the radiation pattern, particularly through the parasitic element terminating impedance, an additional variable not usually available in array

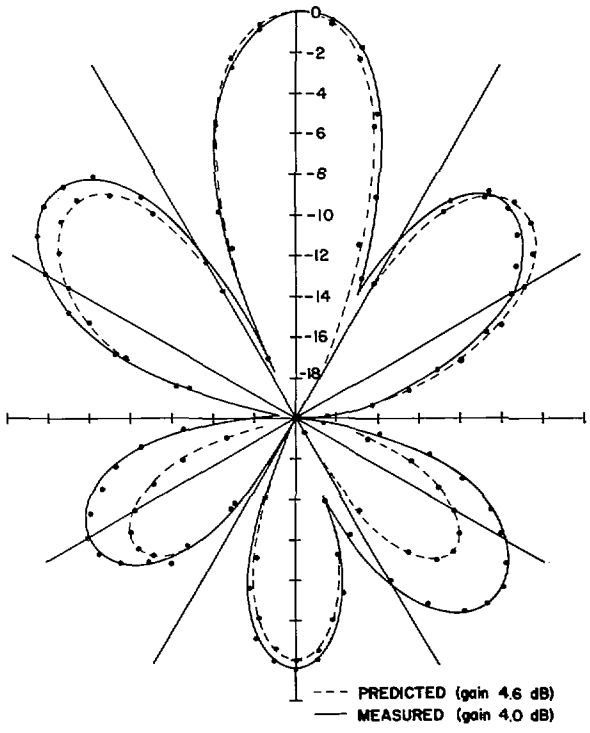

Fig. 5. Comparison of measured and predicted radiation patterns of 400 MHz model.

construction. The heat shield itself has been used as a counterpoise and its irregular shape accounted for by an experimentally determined effective spacing.

ACKNOWLEDGMENT

Special thanks are due Eldon Grindey who fabricated the models and assisted in the testing.

REFERENCES

[1] W. L. Weeks, *Antenna Engineering*. New York: McGraw-Hill, 1968, p. 74.
[2] N. Levanon *et al.*, "A new approach to lightweight radar altimeters," *Proc. IEEE*, vol. 62, pp. 784–792, June 1974.
[3] E. C. Jordan, *Electromagnetic Waves and Radiating Systems*. Englewood Cliffs, N.J.: Prentice-Hall, 1950, p. 375.

Cylindrical Ground-Clutter Shield

CLOVIS S. PEREIRA AND CHEN-TO TAI, FELLOW, IEEE

***Abstract*—A theoretical investigation of the influence of metal shields on antenna radiation patterns is performed. This study allows us to determine the proper dimensions of a circular cylindrical finite perfectly conducting shield placed on the ground around infinitesimal sources located at its axis, in order to reduce the ground-side lobe. Two different methods are applied in this study: 1) integral equation method (IE) and 2) geometrical theory of diffraction (GTD). When the dimensions of the cylindrical shield become very large compared to the wavelength, the first method involves a very large matrix that is impractical for the present computers to handle. Under these circumstances, GTD may be shown to be a very useful approach. For the range of dimensions where both methods are applicable, a comparison between them is made.**

Manuscript received February 12, 1975; revised July 4, 1975.
C. S. Pereira is with the Instituto de Pesquisas Espaciais, São Paulo, Brasil.
C. T. Tai is with the Instituto de Pesquisas Espaciais, São Paulo, Brasil, on leave from the Department of Electrical and Computer Engineering, University of Michigan, Ann Arbor, MI 48104.

I. INTRODUCTION

Echo signals coming from mountains, hills, buildings, and, in general, from any surface on the ground usually disturb and limit the detection capability of a ground-based radar since reflections from a land surface, for example, can be much greater than those from desired targets.

It has already been shown experimentally [1], [2] that ground clutters can be greatly reduced by using a metallic shield. In the present work, with the idea of considering the influence of metal shields on antenna radiation patterns, we investigate theoretically the effects of a circular cylindrical finite perfectly conducting wall around infinitesimal sources mounted over the ground whose conductivity is taken to be infinity.

The two approaches used in this investigation are 1) the integral equation method (IE), 2) Keller's geometrical theory of diffraction (GTD). It should be mentioned that after the completion of this work modification of Keller's theory became available for curved edges [3], [4]. Thus the shortcoming of Keller's theory in the transition region could have been removed if the generalized or the uniform GTD were used.

II. INTEGRAL EQUATION APPROACH

A. Derivation of Integral Equations

The basic formulation in this method involves an integral equation for the current on the cylinder. For all the excitations considered here the integral equations can not be solved in a closed form; they are solved numerically provided the number of sampling points is not too large. The integral equations for three different sources of excitations are described below.

1) *Vertical Infinitesimal Electric Dipole:* As a result of the image theorem, the structure shown in Fig. 1(a) can be replaced by the one shown in Fig. 1(b) as far as the field above the ground plane is concerned. The vector potential due to the dipoles shown in Fig. 1(b) is expressed by

$$A_z^i(\bar{R}) = \frac{\mu_0}{4\pi}\frac{c}{2}\left[\frac{\exp\left(ik\sqrt{\rho^2+(z-h)^2}\right)}{\sqrt{\rho^2+(z-h)^2}} + \frac{\exp\left(ik\sqrt{\rho^2+(z+h)^2}\right)}{\sqrt{\rho^2+(z+h)^2}}\right] \tag{1}$$

where $c/2$ is the current moment of each dipole, ρ and z are the cylindrical coordinates of the observation point P, k is the wave number, and μ_0 is the permeability of the free space.

The surface current density vector $\bar{K}$ is in the z-direction and, by symmetry, it is not a function of the angular coordinate ϕ. Hence by denoting $\bar{K} = K_z(z)\hat{z}$ and designating the unprimed coordinates $R = (\rho,\phi,z)$ for the observation point while the primed ones $R' = (\rho',\phi',z')$ for the source points one has

$$A_z^s(\bar{R}) = \frac{\mu_0}{4\pi} a \int_{-l}^{l}\int_{-\pi}^{\pi} K_z(z')\frac{\exp\left(ik|\bar{R}-\bar{R}'|\right)}{|\bar{R}-\bar{R}'|}\,dz'\,d\phi'. \tag{2}$$

The scattered electric field is related to the vector potential by

$$E_z^s(\bar{R}) = i\omega\left[A_z^s + \frac{1}{k^2}\frac{\partial^2}{\partial z^2}A_z^s\right]. \tag{3}$$